J. Fluid Mech. (1978), *vol.* 84, *part* 1, *pp.* 13–31
Printed in Great Britain

Asymmetric flows and instabilities in symmetric ducts with sudden expansions

By W. CHERDRON, F. DURST
AND J. H. WHITELAW†

Sonderforschungsbereich 80, Ausbreitungs-und Transportvorgänge
in Strömungen, Universität Karlsruhe, Germany

(Received 1 December 1976)

Flow visualization and laser-Doppler anemometry have been used to provide a detailed description of the velocity characteristics of the asymmetric flows which form in symmetric, two-dimensional, plane, sudden-expansion geometries. The flow and geometry boundary conditions which give rise to asymmetric flow are indicated, and the reason for the phenomenon is shown to lie in disturbances generated at the edge of the expansion and amplified in the shear layers. The spectral distributions of the fluctuations in velocity are quantitatively related to the dimensions of the two unequal regions of flow recirculation. It is also shown that the intensity of fluctuating energy in these low Reynolds number flows can be larger than that in corresponding turbulent flows.

1. Introduction

The phenomenon of asymmetric separation of internal laminar flows in the vicinity of an abrupt change in test-section geometry is well known but the corresponding mechanisms that yield this asymmetry are not well understood. The present paper attempts to remedy this situation for low Reynolds number flow through sudden expansions by presenting and discussing the results of flow visualization and velocity and spectra measurements obtained for a range of Reynolds numbers and geometrical arrangements.

An understanding of the nature of low Reynolds number sudden-expansion flows, which can become asymmetric in spite of symmetric test sections and symmetric inlet and outlet velocity profiles, is important for many reasons. It provides, for example, a basis for understanding high Reynolds number flows which appear to exhibit similar characteristics: Abbot & Kline (1962) observed, by visualization methods, the asymmetry of the turbulent flow downstream of a plane, symmetric sudden expansion and Smyth (1976), with a laser-Doppler anemometer, has provided quantitative evidence of the asymmetry for one geometrical arrangement. Although physical reasons for the occurrence of the asymmetric flows are not provided in the aforementioned publications, the results suggest that the origin of the asymmetry is related to the shear layers and to coherent flow structures embedded in the random velocity fluctuation. Winant & Browand (1974) have shown in a recent publication that such structures exist in shear layers and can interact with each other, yielding

† Permanent address: Mechanical Engineering Department, Imperial College, London.

phenomena that dominate the flow characteristics. The present results, obtained in low Reynolds number flows, also show the importance of coherent eddy-like structures. In this case the eddies originate in two shear layers but are interdependent because of confinement and so strongly influence the characteristics of the flow. This can have important consequences for related turbulent flows, including those formed in fluidic devices.

The detailed velocity measurements are also important in that they provide a basis for the testing of calculation methods. The present symmetric geometries, even with Reynolds numbers which correspond to laminar flow, result in stable asymmetric flows, in spite of symmetric inlet and outlet velocity profiles. Thus they pose a new important problem for numerical solutions of differential conservation equations. It is likely that the solution of time-dependent equations which take account of flow disturbances will be required to treat such flows numerically.

In a previous contribution to this topic, Durst, Melling & Whitelaw (1974) reported velocity profiles and spectra of the velocity fluctuations measured with a laser-Doppler anemometer along the centre-line of a test section with a sudden expansion of ratio 3:1 and with aspect ratio 9·2:1 after the expansion. At very low values of the Reynolds number, the flow was apparently two-dimensional in the central region and the results agreed with calculated values obtained by solving the corresponding steady two-dimensional forms of the partial differential equations representing conservation of mass and momentum. The measurements showed that at higher Reynolds numbers the flows became asymmetric with separation regions of unequal size on opposite sides of the symmetric expansion; a third recirculation region was observed at still higher Reynolds numbers and flow oscillations of increasing amplitude were reported as the Reynolds number was further increased.

No physical explanations were given for these observations but detailed results were presented to quantify the asymmetric velocity fields and the frequencies of the flow oscillations. The range of velocity and spectra measurements, obtained with a laser-Doppler anemometer, has been extended in the present paper to test sections of different expansion and aspect ratios and flow-visualization techniques have again been employed to assess quantitatively the onset of flow asymmetry as a function of geometry and Reynolds number. Smoke patterns in the vicinity of the regions of recirculation were recorded with a high-speed camera and provide useful photographs of flow structure quantified by the measurements with the laser-Doppler anemometer. These new results support physical mechanisms which are postulated to explain the phenomena observed here and in previous work.

The extensive literature relating to axisymmetric separated flows includes the papers of Macagno & Hung (1967), Lavan & Shavit (1971), Iribarne *et al.* (1972) and Back & Roshko (1972) and is relevant to the present investigation because it reveals the existence of flow instabilities. Iribarne *et al.*, for example, observed wavelike disturbances in their pipe jet over a wide range of Reynolds numbers. Unlike the present flows, however, the measured mean velocity profiles in the axisymmetric flows were themselves symmetric. Previous investigations of two-dimensional, plane separated flows have tended to concentrate on backward-facing steps, for example Mueller & Leary (1970) and Goldstein *et al.* (1970), and obstacles such as roughness ribs, for example Oka & Kostic (1971). In general, these investigations were concerned with time-average properties such as the length of recirculation regions and

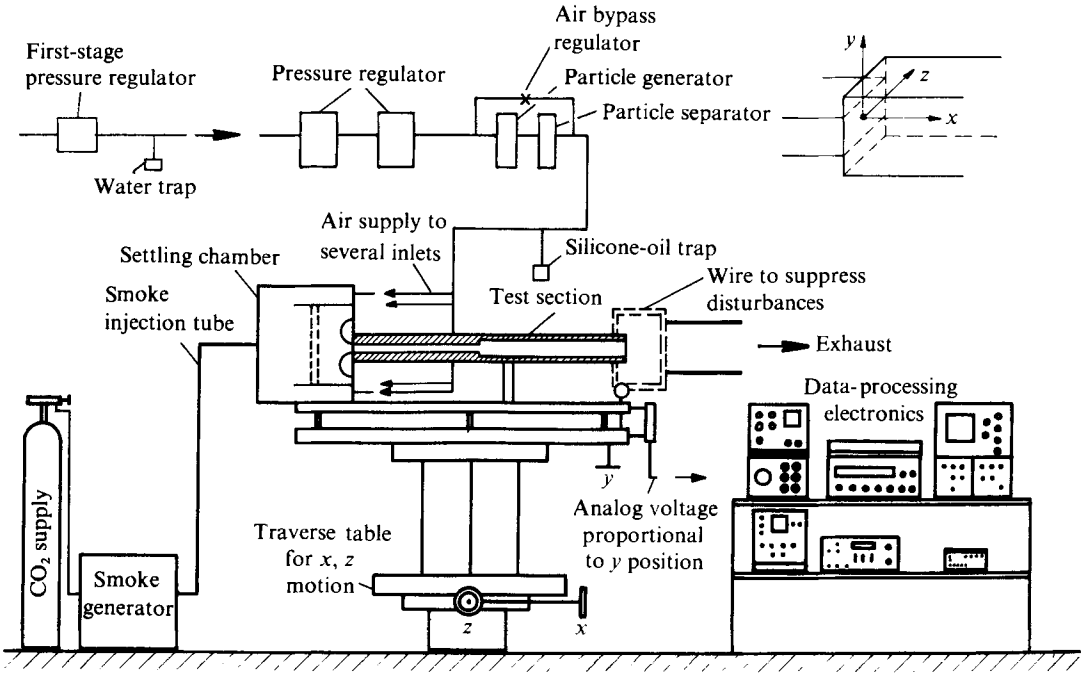

FIGURE 1. Schematic representation of experimental test rig.

employed flow-visualization methods and other means of investigation which presumed that the flow was two-dimensional. The three-dimensional nature of the flow over two-dimensional geometries was, however, demonstrated by the flow-visualization experiments of Goldstein *et al.*

The flow instabilities observed in sudden-expansion flows are related to those observed in free flows, for example by Sato (1959), although plane sudden-expansion flow is further complicated by the special nature of interaction between the two shear layers caused by the confinement of the flow. Sato deduced that, in two-dimensional jets, the flow oscillations observed in the vicinity of the shear layers are caused by velocity fluctuations, of small amplitude, which themselves originated near the nozzle exit plane. Fully developed nozzle velocity profiles led to antisymmetric shedding and undeveloped profiles to symmetric shedding. These findings are supported by the more recent work of Rockwell & Niccolls (1972), for fully developed nozzle velocity profiles, and of Beavers & Wilson (1970), for undeveloped profiles. The relationship between the oscillations observed in free flows and those in two-dimensional, plane sudden-expansion flows will be demonstrated. It may be expected that where flow characteristics, such as those caused by the small dimensions of the present ducts, lead to interaction between shear layers, vortex shedding will be antisymmetric. The extensive literature relating to the numerical representation of unsteady flows has been described, for example, by Clements & Maull (1976) but does not include solutions for the present geometrical arrangements. The book by Betchov & Criminale (1967, p. 109) does, however, suggest a mechanism of disturbance amplification in shear layers which has common features with the results of the present investigations.

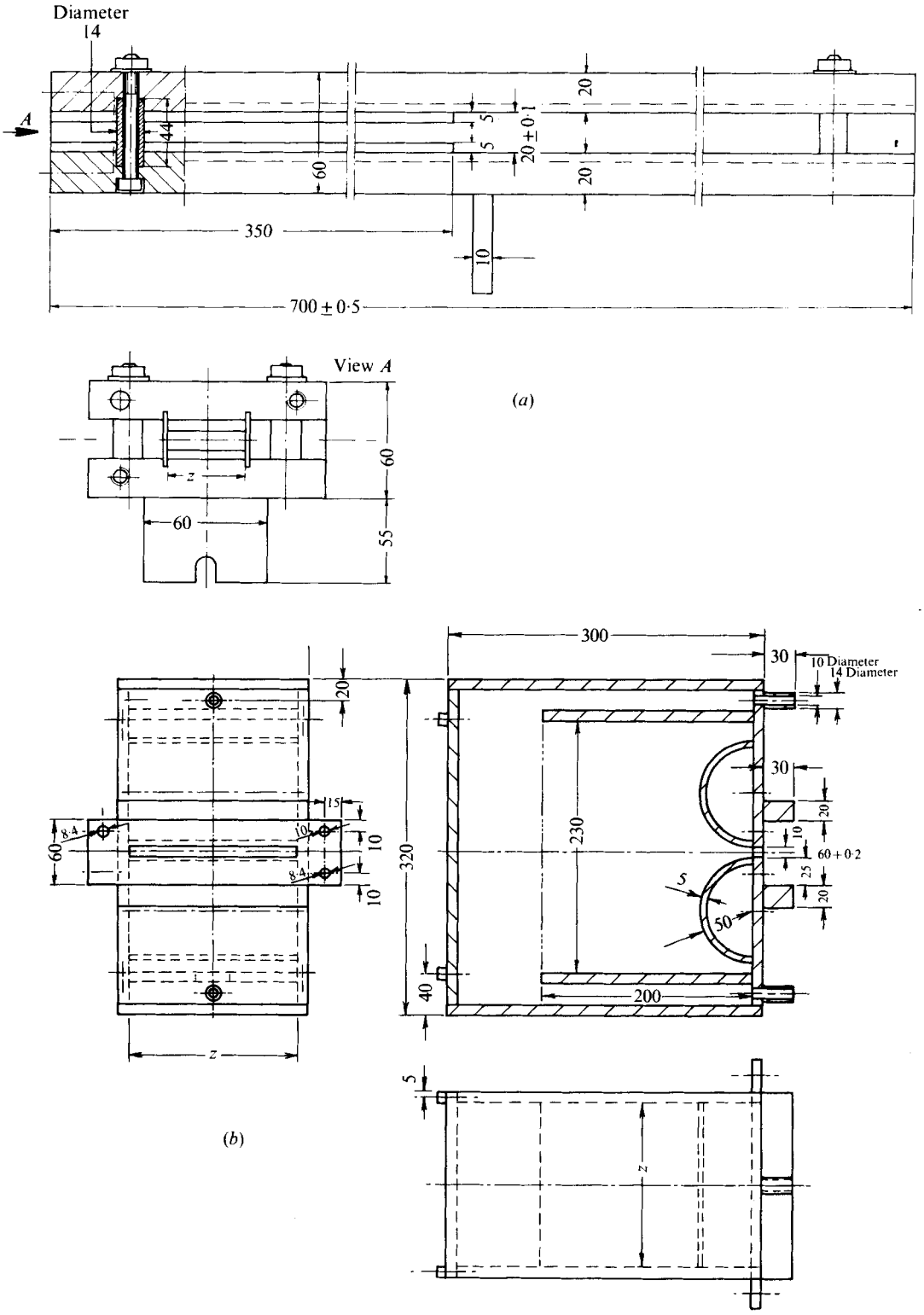

FIGURE 2. Dimensions and construction of (*a*) two-dimensional channels with different aspect ratios and (*b*) plenum chamber. Aspect ratio = 1, 2, 4 or 8. z = 20, 40, 80 or 160 mm. All measurements in mm.

In this paper, the geometrical details of the sudden-expansion arrangements are provided in the next section together with essential information on the flow-visualization equipment and laser-Doppler instrumentation. The results of the flow-visualization experiments are presented in § 3 and the velocity measurements in § 4. Where possible, the results are related to previous investigations and the physical implications stated and discussed.

2. Flow configurations and instrumentation

2.1. *Arrangements of flow configurations*

A schematic representation of the experimental arrangement is shown in figure 1. The figure shows that compressed air was supplied through a pressure regulation system which allowed the flow rate to be maintained constant to within 0·3 % over extensive periods of time to an arrangement of silicone-oil atomizers which acted as particle generators. The air at the exit from the atomizer carried silicone-oil droplets suitable for light scattering, 99 % of their population having diameters less than 3 μm. The concentration of particles was sufficient to allow the use of a frequency-tracking demodulator with an effectively continuous Doppler signal. The seeded air passed to a settling chamber connected by a contraction to the test section. Each test section had its own settling chamber and contraction to ensure well-controlled inlet flow conditions. The test section was fixed to a three-dimensional traverse arrangement which allowed the measuring position to be located to within 5×10^{-5} m in the x and z directions and to within 10^{-5} m in the y direction.

The test sections were manufactured with glass side walls and with other parts machined from Perspex. The construction is shown in figure 2(*a*) and was basically the same for all expansion and aspect ratios. Detailed velocity measurements were obtained with an expansion ratio of 2 and with an aspect ratio of 2; flow-visualization experiments made use of aspect ratios of 1, 2, 4, and 8 and expansion ratios of 2 and 3.

The flow entered the plenum chamber through a number of pipes. It was guided to the back of the chamber and passed through several screens before reaching the contraction, which had the dimensions shown in figure 2(*b*). The velocity profiles at the end of the contraction were uniform apart from thin regions of boundary-layer development at the front and back walls. In the plane of the sudden expansion, the velocity profiles were fully developed and parabolic in form even at the highest Reynolds number investigated.

The outlet region of the test sections was surrounded by wire-mesh cages which prevented any significant influence of fluctuations in the surrounding air on the flows under examination.

2.2. *Flow-visualization instrumentation*

An oil evaporation arrangement, which made use of carbon dioxide as the driving gas and a small electric heater, supplied scattering particles in the form of oil droplets to the plenum chamber as shown in figure 1. The flow rate of oil smoke was controlled by a pressure regulator to allow the following four visualization techniques.

(i) To obtain time-averaged information on the shape of the regions of recirculation, smoke was introduced until these regions were filled. The smoke supply was then

turned off with the result that the smoke cleared from the regions of non-recirculating flow. Photographs, like that in figure 3(*a*) (plate 1), were then taken with exposure times of approximately $\frac{1}{30}$ s.

(ii) To obtain time-averaged information on the flow inside and around the regions of recirculating flows, smoke was introduced until the recirculation regions partly filled, as indicated on figure 3(*b*) (plate 1). The exposure times were again of the order of $\frac{1}{30}$ s.

(iii) To provide information on the entire flow field at any instant, smoke was introduced until the separation regions were filled then the smoke supply was turned off. Time exposures of the order of $\frac{1}{500}$ s were used to obtain photographs like that in figure 3(*c*) (plate 1).

(iv) To examine the apparent vortex formation† and the subsequent eddy growth, smoke was supplied through small injection nozzles. The result, as indicated on figure 3(*d*) (plate 1), was localized smoke streaks, obtained with an exposure time of $\frac{1}{500}$ s.

In all cases, a 2 kW halogen lamp and a slot mask were employed to provide local illumination over a 2·5 mm wide strip. A 35 mm single-lens reflex camera with 400 ASA film was used to obtain the still photographs; the developing procedure increased the effective film speed to 1400 ASA. Ciné films were obtained with a 16 mm camera (Vinten HS250) and a film speed of 250 frames/s.

2.3. *Laser-Doppler measurements and data-processing system*

The laser-Doppler anemometer employed in the present investigation was operated in the fringe mode with an optical arrangement similar to that used by Durst *et al.* (1974). The details of the arrangement depended on where the particular measurements were made: for example a 5 mW He–Ne laser was used for experiments carried out at Imperial College and a 15 mW He–Ne laser for those at the University of Karlsruhe. The focal length of the transmission lenses (200 mm) resulted in an intersection volume of the two light beams with major and minor axes, at the $1/e^2$ intensity locations, of approximately 0·2 mm and 1·1 mm. The arrangement of the light collecting system reduced the smaller dimension to approximately 0·15 mm and the finite discrimination of the electronic-processing system reduced both dimensions to approximately 0·1 mm and 0·5 mm.

The Doppler signal from the photomultiplier (EMI 9558) was monitored on an oscilloscope. Two frequency-tracking demodulators (BBC-Goerz LSE 01 and DISA 55L20) were used to process the Doppler signals at different times: the results from the two instruments proved to be identical. The demodulated signal, at the output from a frequency-tracking demodulator, was processed by a time-domain analyser (Solartron JM1860) to determine the mean velocity and a true r.m.s. meter (DISA 55D35) to determine the r.m.s. value of the velocity fluctuations. These values were supplied to the y co-ordinate of an x, y recorder: the x co-ordinate of the recorder was driven by an analog signal which corresponded to the y position in the test section. The digital output of the tracker, corresponding to individual velocity values, was supplied to a counter, for more accurate results.

† The work of Hama (1962) suggests that flow visualization of this type can lead to the misinterpretation of coherent disturbances as vortices.

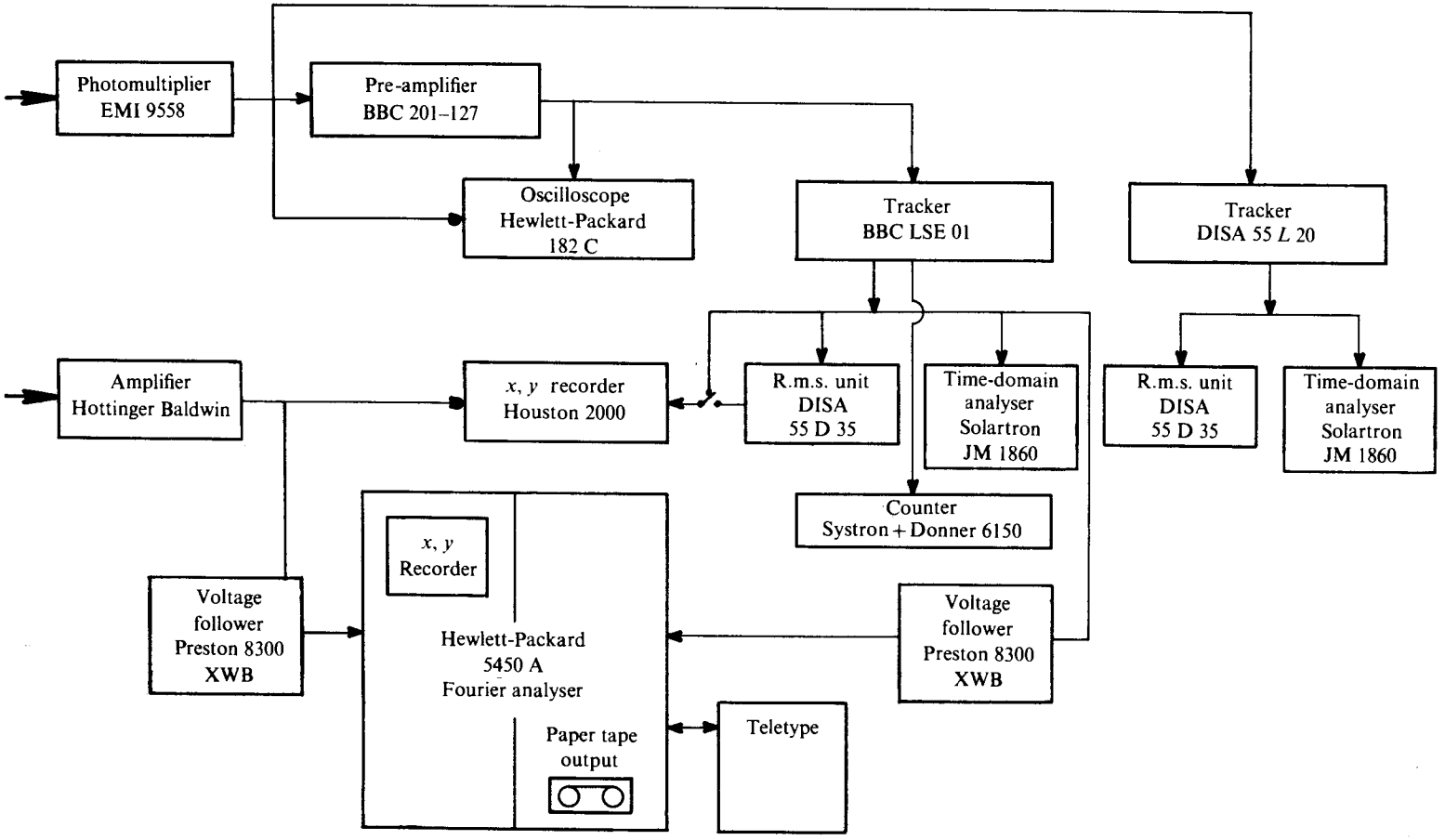

FIGURE 4. The data-processing system.

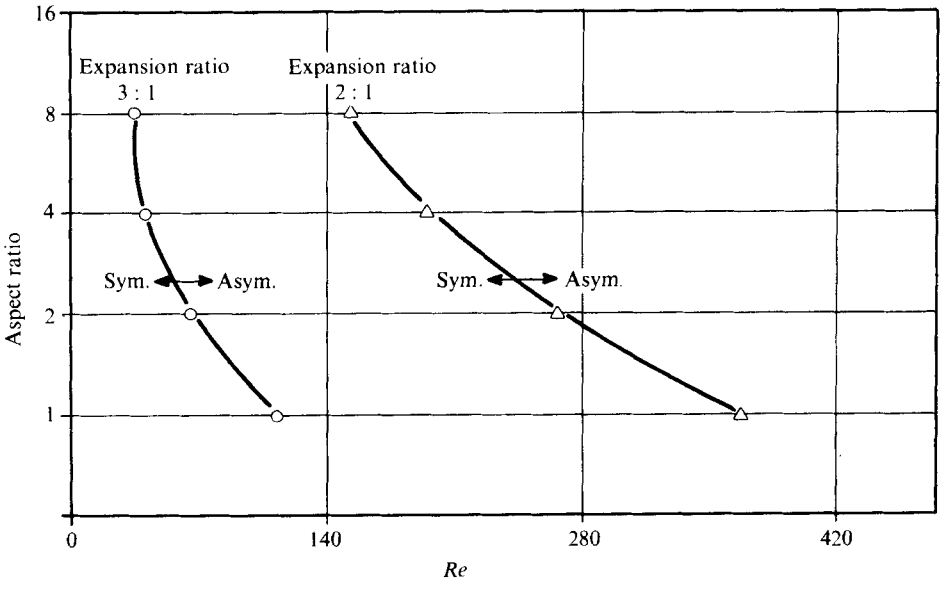

FIGURE 6. Boundaries of symmetric and asymmetric flow.

To obtain frequency spectra, the analog signal from the BBC Goerz tracker was supplied to a fast Fourier analyser (Hewlett Packard 5440A). The output from the analyser was available on an x, y plotter for diagnostic purposes and on paper tape for subsequent computer processing. This is indicated on figure 4, where the complete signal-processing arrangement is shown in block-diagram form. In general, the instrumentation conformed to the design principles of Durst, Melling & Whitelaw (1976).

3. Flow-visualization results

3.1. *Mean flow characteristics*

The flow-visualization equipment described in §2.2 was used first to obtain time-averaged information on the different flow regimes near the sudden expansion. The photographic records obtained with an expansion ratio of 3 were similar to those of Durst *et al.* (1974) and were extended to an expansion ratio of 2. Figure 5 (plate 2) shows that, for an expansion ratio of 2 and an aspect ratio of 8, the regions of recirculating flow on the two sides of the duct are identical in size but increase in length as the Reynolds number, based on the maximum velocity in the region of the expansion and the corresponding duct height, increases from 110 to 150. For higher Reynolds numbers, the flow becomes asymmetric and this is shown in figure 5(*c*) for $Re = 500$. The change from symmetric to asymmetric flow occurred over a relatively small range of Reynolds numbers: at a value of 150 the flow was symmetric but at 185 it was asymmetric with a flow pattern similar to that in figure 5(*c*). The observation of this transition from symmetric to asymmetric flow for a range of aspect ratios and for expansion ratios of 2 and 3 allowed the construction of figure 6, which maps the regions of symmetric and asymmetric flow. It is clear from the figure that a decrease in the aspect and expansion ratio has a stabilizing effect which extends the range of Reynolds numbers over which symmetric flow can exist.

The results shown in figures 3 and 5 were obtained with the illuminated slot in the x, y plane. Figure 7 (plate 3) shows a series of photographs taken with the illuminated slot in the x, y and y, z plane at a series of x positions. The test section had an expansion ratio of 2 and an aspect ratio of 2. The Reynolds number was 415 and, as can be seen from the end-view photographs, the flow was asymmetric. The time exposure for the end-view photographs was $\frac{1}{500}$ s, hence they represent snapshots of the time-varying flow. This is indicated by the three pictures shown for the same downstream distance. All photographs indicate the three-dimensional nature of the flow, which is similar to that obtained by Durst *et al.* in their channel and may be readily related to the secondary flow patterns described by Goldstein *et al.* (1970); it exists for all aspect ratios investigated here.

A series of photographs was taken at small time steps after the flow was started in order to determine the manner in which the flow became established. It showed that vortices form first in the corners behind the steps and grow rapidly to establish the main region of recirculating flow. When this primary flow pattern has been established, the three-dimensional secondary flows gradually build up until a steady state is reached. The regions of recirculation in the x, z plane are initially strongly asymmetric but tend to become more symmetric with increasing time. Figure 8 (plate 4) shows a typical photograph of the flow with the illumination slot in the x, z plane at a y location close to the wall, the test section and Reynolds number corresponding to those of figure 5(*c*). It reveals corner eddies which are of similar length to the larger recirculation region of figure 5(*c*) and also shows two eddies located immediately behind the step and of the order of one step height in length. The flow is clearly not symmetric at this y value and time.

Visualization was also used to assess the influence of geometrical and flow imperfections on the symmetry of the flow. It was found that placing one step at a different x location from the other resulted in asymmetric flow with the smaller recirculation region associated with the upstream step. Similarly, if the flow on one side of the approaching flow was made to separate immediately upstream of a sudden expansion, the recirculation region was always shorter on the side where the flow was forced to separate. All the test sections used for the measurements described in this report were constructed and assembled with particular care: as a consequence, the shorter region of recirculation could occur and exist in a stable manner on either side; it could, however, be forced from one side to the other as described by Durst *et al.* (1974).

3.2. *Flow oscillations*

The results of the previous section were supplemented by a photographic examination of the eddy-like structure of the flow. This series of experiments was intended to provide information on the formation of the asymmetric flow patterns and about the flow oscillations previously observed at the higher values of the Reynolds number. The exposure time for most photographs was of the order of $\frac{1}{500}$ s and thus about ten times faster than the frequency used for stroboscopic observations of the flow.

Typical results are shown on figure 9 (plate 5), which presents smoke patterns recorded by the visualization technique described in §2 which is appropriate to the observation of instantaneous flow patterns. The vortex-like structures, corresponding

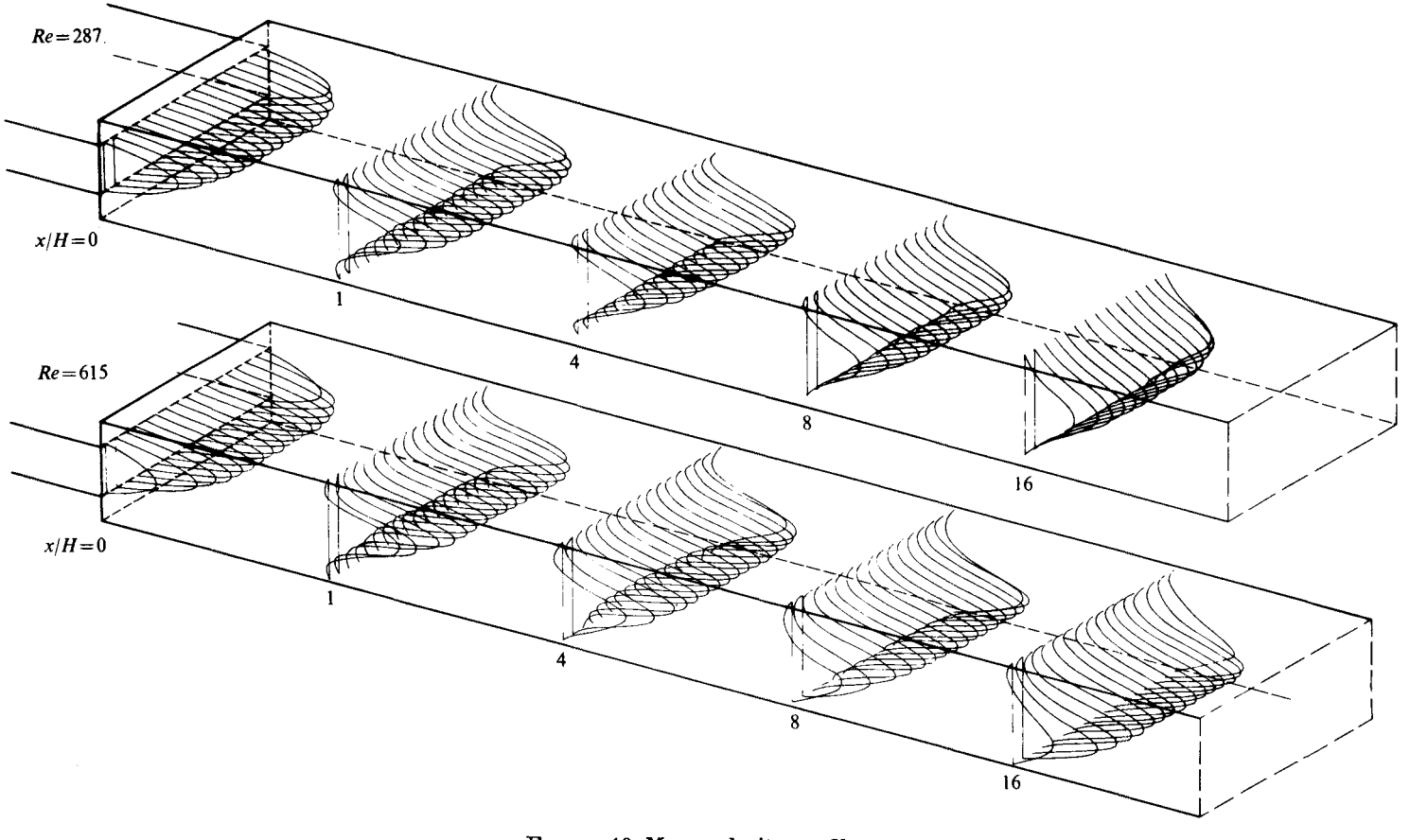

FIGURE 10. Mean velocity profiles.

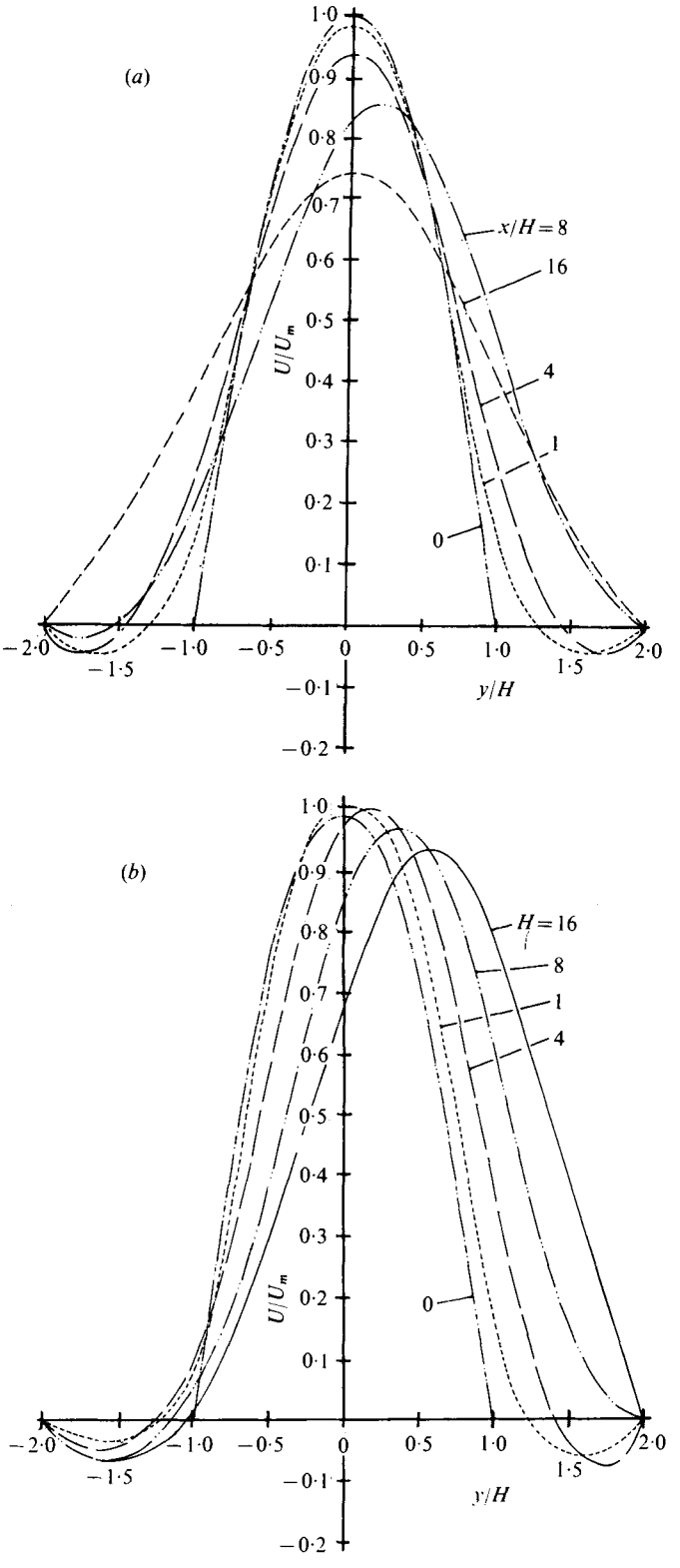

FIGURE 11. Velocity profiles in the symmetry (x, y) plane for an aspect ratio of 2, an expansion ratio of 2 and a Reynolds number of (*a*) 287 and (*b*) 615.

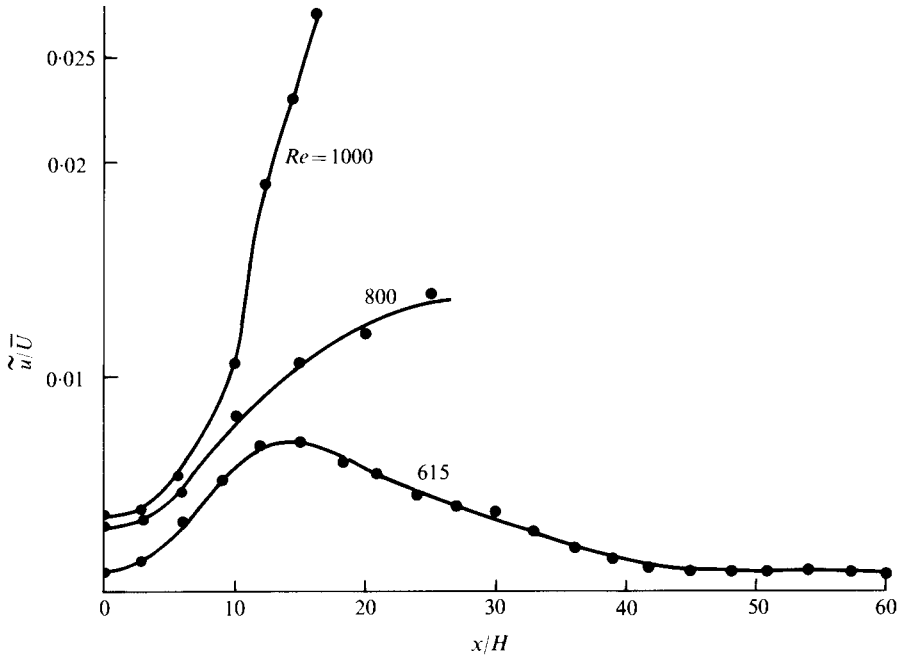

FIGURE 12. Normalized r.m.s. velocity fluctuations on axis of duct for three Reynolds numbers.

to the two shear layers, are similar to those observed in free jets by Sato (1959) and Rockwell & Niccolls (1972) but are asymmetric owing to the confined nature of the flow and the consequent interaction between the two vortex-like patterns. The flow photographs relate to an expansion ratio of 2 and demonstrate that for a wide range of geometries and flow conditions similar patterns exist which are, for the present initial velocity profiles, specified by the asymmetric flow regime of figure 6. In regions of symmetric flow, the vortex-like structure began to form but was damped and rapidly gave way to streamline flow. Many observations, similar to those of figure 9, indicate that the vortex-like structure stemmed from small perturbations at the edge of the expansion. The disturbances grow to form the flow patterns which are shed alternately from the two shear layers and these may coalesce when a limiting size, dictated by the bulk flow velocity and channel dimensions, is attained. The direct relationship between the wavelength of the apparent eddy structure and the length of the shorter recirculation region, deducible from figure 9, indicates that the asymmetry of the mean flow and the vortex-like structure are linked. The shorter region of separation corresponds to one wavelength of the flow oscillations and the longer region to three.

4. Quantitative velocity information

4.1. *Mean velocity distributions*

The instrumentation described in §2.3 was used to obtain detailed distributions of local mean velocity at Reynolds numbers of 287 and 615 in the duct of aspect and expansion ratio 2. Detailed records of these data, which may be usefully compared

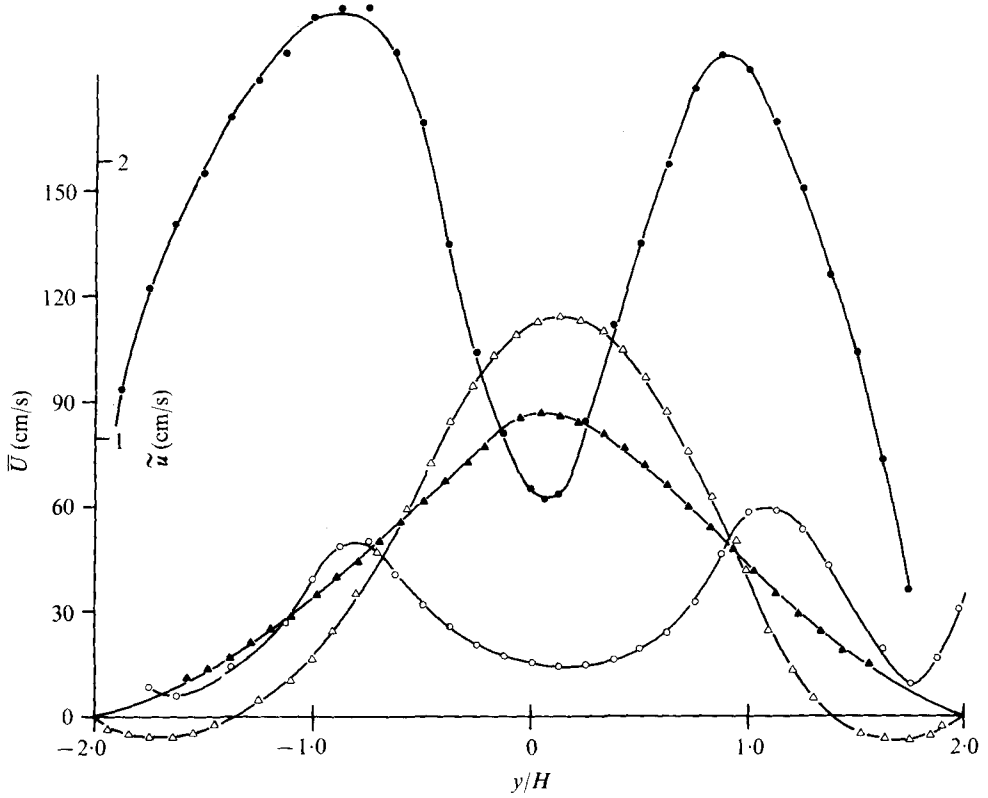

FIGURE 13. Mean (triangles) and r.m.s. (circles) velocity profiles in the symmetry (x, y) plane for a Reynolds number of 800, an aspect ratio of 4 and an expansion ratio of 2. ●, ▲, $x/H = 4$; ○, △, $x/H = 0{\cdot}5$.

with the results of three-dimensional calcuation methods, are available from the first author on request. Related, but less extensive, information was provided by Durst *et al.* (1974) for the duct of aspect ratio 9·2 and expansion ratio 3.

Figure 10 presents, in isometric projection, the development of the velocity profiles for two Reynolds numbers that correspond, as can be seen from figure 6, to the range in which asymmetric flow patterns were observed by flow-visualization techniques: the asymmetry about the x, z plane at $y = 0$ is confirmed by the measured velocity profiles. This asymmetry occurs in spite of symmetric inlet profiles and the symmetry of the test-section geometry. With boundary conditions of this type, a symmetric flow is usually expected and presumed in flow predictions, where half a test section is considered for the solution domain. Calculations performed with presumed symmetric boundary conditions would, of course, lead to erroneous results for the present flows. Figure 11 presents the velocity profiles at $z = 0$ and allows the recirculation to be identified more readily. It also shows that the lower Reynolds number flow has returned to a symmetric velocity distribution at a value of x/H of 16. The higher Reynolds number flow, on the other hand, still has a very asymmetric velocity distribution at $x/H = 16$ and has almost maintained the initial maximum velocity over the range of measurements. The discussions in §§ 3.1 and 3.2 relate the asymmetry of the flow to the vortex structure and confirm the faster decay of the eddy structure

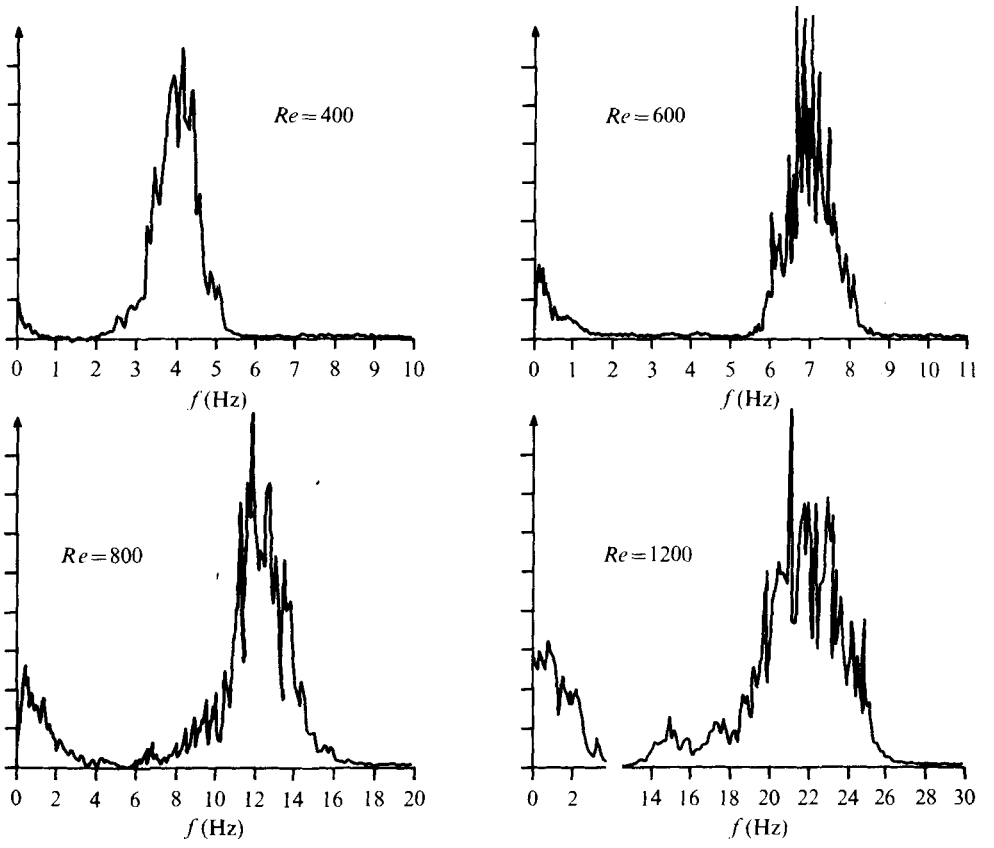

FIGURE 14. Spectral distribution of fluctuating energy for an expansion ratio of 2 and an aspect ratio of 8.

at the lower Reynolds number. This qualitative observation is confirmed by the measurements.

4.2. *Velocity fluctuations*

Measurements of the r.m.s. values of the velocity fluctuations corresponding to the measured values of the mean velocities of the previous section were obtained and provide a measure of the strength of the vortex-like structure revealed by the visualization experiments. In addition, the spectral distribution of the energy of fluctuation was determined to provide quantitative information on the frequency at which disturbances are shed from the shear layer; photographs, of which figure 9 provides a sample, suggested that the relevant range of frequencies for an expansion ratio of 2 is from 5 to 20 Hz.

Figure 12 presents distributions of the root mean square of the longitudinal velocity fluctuations normalized with the local mean velocity obtained along the axis of the test section for Reynolds numbers of 615, 800 and 1000. General features of the flow may be deduced from this figure but, as will be shown, the cross-stream profiles are not uniform, and distributions for different values of y would be quantitatively different. It is clear, however, that the energy of fluctuation increases with the Reynolds number and, for the present range of Reynolds numbers, it will reach a

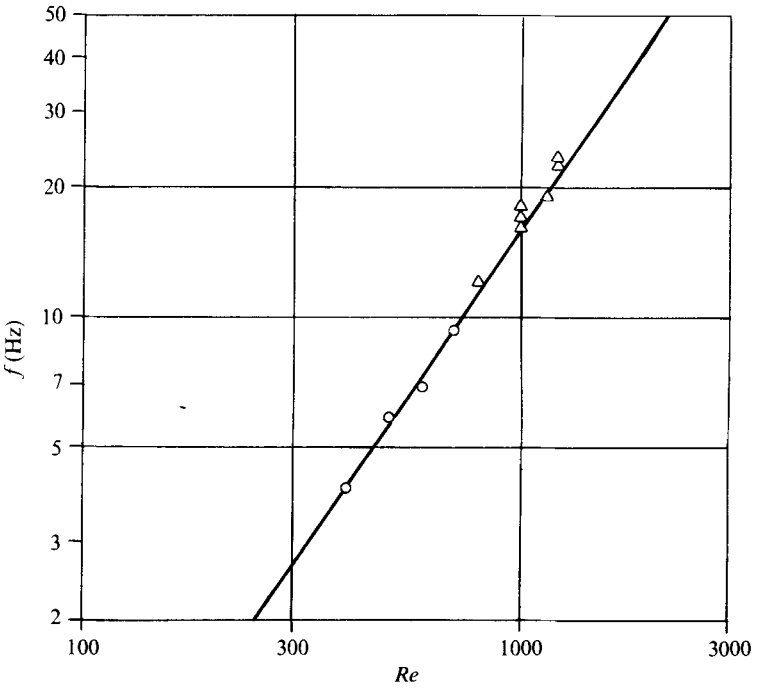

FIGURE 15. Predominant frequency as a function of Reynolds number. △, aspect ratio = 2; ○, aspect ratio = 8.

maximum value and decrease to zero at some location far downstream. The damping of the disturbances further downstream stems from the combined influence of viscosity and the duct walls. Cross-stream profiles of the r.m.s. value of the velocity fluctuations and the corresponding mean velocity profiles are presented in figure 13 for a Reynolds number of 800. Two maxima, coincident with the locations of the inflexions in the mean velocity profiles, exist on either side of the centre-line values in figure 12 and represent fluctuation intensities $\tilde{u}/U$ of approximately 0·017 at the upstream location and 0·07 at the downstream location. The magnitude of these intensities, caused by the vortex-like nature of the flow, is even greater for a Reynolds number of 1000 and significantly larger away from the wall than might be expected in a turbulent duct flow.

The spectral distribution of the energy of fluctuation obtained in the duct with an expansion ratio of 2 and aspect ratio of 8 is plotted on figure 14 as a function of Reynolds number. The measurement location in the flow does not influence the general shape of these distributions although small differences in the distribution of energy may occur: the same characteristic frequencies were observed at all locations in the flow where the energy fluctuation level was sufficient to permit recognizable spectra to be obtained. The figure demonstrates that most of the fluctuation energy is associated with a frequency which increases from 4 Hz at a Reynolds number of 400 to 22 Hz at a Reynolds number of 1200. A much smaller concentration of energy is also present at a frequency of approximately 0·05 of the predominant frequency. Spectra were more readily measured with the larger aspect ratio but were also obtained for an aspect ratio of 2; figure 15 shows the variation of the predominant frequency, as a function of Reynolds number, for both aspect ratios.

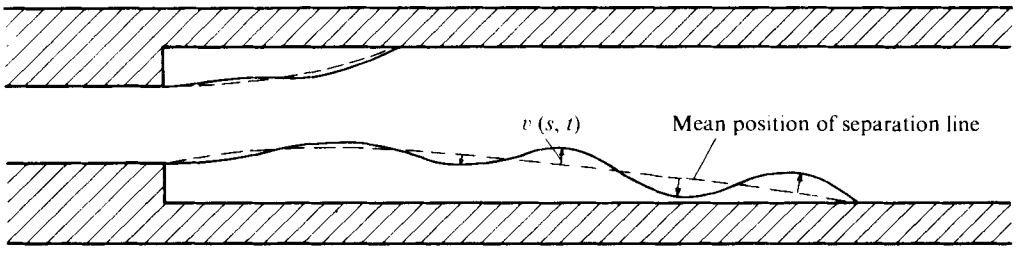

FIGURE 16. Flow oscillations perpendicular to mean position of separation line.

5. Discussion of results

The results of the previous section and the related information of Durst *et al.* (1974) demonstrate that symmetric flows can exist in two-dimensional, plane, symmetric, sudden-expansion ducts for only a limited range of Reynolds numbers. At higher Reynolds numbers, the small disturbances generated at the lip of the sudden expansion are amplified in the shear layers formed between the main flow and the recirculation flow in the corners. The result is a shedding of eddy-like patterns which alternate from one side to the other with consequent asymmetry of the mean flow, particularly of the dimensions of the two regions of recirculation. Although the flow is three-dimensional, its major features can be understood by considering the interaction of two-dimensional shear layers.

The amplication of disturbances in shear layers has been referred to by Betchov & Criminale (1967, pp. 99 ff.) and the consequent existence of oscillations maintained by appropriate feedback mechanisms has been postulated by Martin (1974) and Martin, Naudascher & Padmanabhan (1975) for single regions of recirculating flow. The same mechanisms apply to the present flows but are complicated by the interaction between the two shear layers. The vortex-like patterns, for example those in figure 9, influence the flow in the opposite half of the duct through velocity fluctuations, normal to the main flow, which extend from each shear layer to the duct centre. Indeed, the flow can generally exist only if the fluctuating normal velocities originating from one shear layer are out of phase with those from the other. As a result, the shedding in vortex-like flow patterns is antisymmetric.

The antisymmetric shedding causes asymmetric mean flow patterns, as shown in figure 11, and hence recirculating flow regions of unequal length. Owing to the existence of velocity oscillations perpendicular to the mean separation line, the flow in the separated regions is continuously entrained into the shear layers and replaced by fluid from the main flow. In order to maintain separated regions that are stable, as far as the average flow properties are concerned, the time-averaged inflow must equal the time-averaged outflow. An additional requirement for stable recirculating regions is imposed by the 'locking-on' condition postulated by Martin (1974), which states that only an uneven number of complete oscillation cycles will feed back the correct in-phase disturbance to the lip of the step from which separation occurs. The major contribution to this disturbance stems from the departure, at the end of the separation region, of eddies with their entrained fluid. Separation lengths corresponding closely to an integral number of complete oscillation cycles maintain these self-induced oscillations. Figure 16 demonstrates the arrangement of the instantaneous

and time-averaged separation lines with the larger recirculation region corresponding to three cycles.

In general the lengths of the recirculation regions are close to multiples of the wavelength of the disturbance and are functions of the maximum velocity, the initial profile shape and the step height; they are unequal to accommodate the anti-symmetric shedding. The present measurements show that the most probable multiple for the longer separation region is three but this can vary from one configuration to another and, on occasions, with time. The length of the smaller region of re-circulation always corresponds to a single wavelength since this is the most stable arrangement.

The magnitude of the predominant frequency, in contrast to the constant values of the wavelength of the vortex-like patterns and the length of the recirculation zones, is directly dependent upon the maximum velocity and the shape of the profiles in the plane of the expansion. The dependence upon the maximum velocity has the form of $U_m^{\frac{3}{2}}$, as indicated by figure 15: the change in aspect ratio used to obtain the results in this figure has no direct influence on the frequency–velocity relationship. The present results were obtained with an initial velocity profile which was fully developed; as a consequence, the initial disturbances were amplified more strongly than those of Durst *et al.* (1974), who used an undeveloped initial profile. The frequencies observed with the thinner initial boundary-layer thickness were of the order of ten times greater than those with the thicker initial layer, which is compatible with the difference in non-dimensional boundary-layer thickness and agrees with predictions of flow instability calculations. The expansion ratios of the two experiments were not the same but this influenced the shape of the recirculation regions, and the number of wavelengths forming the larger one, rather than the frequency–velocity relationship of the flow oscillations.

An implication of the independence of the frequency and wavelength of the step height of the sudden expansion is that, for a given initial profile, expansions which are too large will give rise to jet-like flow with no reattachment while for expansion dimensions corresponding to a step height of around one wavelength the reattachment will be unstable.

The present results can be readily linked to those observed in free flows by the analysis of Michalke (1971), whose analytical mean velocity profiles have been matched to the present measurements at $x/H = 1$ to determine values of the parameter ϑ used in his instability calculations. This parameter, together with the measured frequency of the flow oscillations and the value of the maximum velocity, allows the determination of a characteristic Strouhal number of approximately 0·11. According to Michalke's results, the amplification of shear-layer distrubances reaches a maximum in the vicinity of this Strouhal number. This provides further justification for the hypothesis that the asymmetric flow patterns observed in two-dimensional, plane, sudden-expansion geometries are entirely controlled by flow instabilities, i.e. the amplification of self-induced disturbances from the lip of the expansion in the shear layer of the separated-flow regions.

It is also of interest to note that, with the larger aspect ratios, in the vicinity of the downstream end of the longer region of recirculating flow two discrete frequencies were observed in some spectral distributions. The second peak was located at a frequency which was always smaller than the main frequency by a factor correspond-

ing to the number of wavelengths of the flow oscillations defining the longer recirculation region. This secondary spectrum contained less energy than the spectrum of the predominant frequency. Investigations showed that lower frequency oscillations may be associated with a tendency for the larger region of recirculation to entrain more mass than it can accept at a certain instant without changing size. As a consequence, a lower-energy disturbance is set up at a frequency corresponding to the length of the recirculating region and may be interpreted as a periodic discharge of mass from this region.

The work was made possible by financial support from the Deutsche Forschungsgemeinschaft and the Science Research Council. The collaboration between Imperial College and the University of Karlsruhe was assisted by a grant to one of us (WC) from the Deutscher Akademischer Austauschdienst. We are also grateful to Dr W. Martin for useful discussions. Miss G. Bartman and Mrs M. Cherdron were helpful in preparing the final version of the paper.

REFERENCES

ABBOT, D. E. & KLINE, S. J. 1962 Experimental investigations of subsonic turbulent flow over single and double backward facing steps. *J. Basic Engng, Trans. A.S.M.E.* D **84**, 317.

BACK, L. H. & ROSHKO, E. J. 1972 Shear-layer flow regions, wave instabilities and reattachment lengths downstream of an abrupt circular channel expansion. *J. Appl. Mech.* **39**, 677.

BEAVERS, G. S. & WILSON, T. A. 1970 Vortex growth in jets. *J. Fluid Mech.* **44**, 97.

CLEMENTS, R. R. & MAULL, D. J. 1975 The representation of sheets of vorticity by discrete vortices. *Prog. Aerospace Sci.* **16**, 129.

BETCHOV, R. & CRIMINALE, W. O. 1967 *Stability of Parallel Flows.* Academic Press.

DURST, F., MELLING, A. & WHITELAW, J. H. 1974 Low Reynolds number flow over a plane symmetrical sudden expansion. *J. Fluid Mech.* **64**, 111.

DURST, F., MELLING, A. & WHITELAW, J. H. 1976 *Principles and Practice of Laser-Doppler Anemometry.* Academic Press.

GOLDSTEIN, R. J., ERIKSEN, V. L., OLSEN, R. M. & ECKERT, E. R. G. 1970 Laminar separation, reattachment and transition of the flow over a downstream-facing step. *J. Basic Engng, A.S.M.E.* D **92**, 732.

HAMA, F. R. 1962 Streaklines in a perturbed shear flow. *Phys. Fluids* **5**, 644.

IRIBARNE, A., FRANTISAK, F., HUMMEL, R. L. & SMITH, J. H. 1972 An experimental study of instabilities and other flow properties of a laminar pipe jet. *A.I.Ch.E. J.* **18**, 689.

LAVAN, Z. & SHAVIT, G. 1971 Recirculation patterns in confined laminar jet mixing. *Israel J. Tech.* **9**, 51.

MACAGNO, E. O. & HUNG, T. K. 1967 Computational and experimental study of a captive annular eddy. *J. Fluid Mech.* **28**, 43.

MARTIN, W. W. 1974 Anwendung der hydrodynamischen Stabilitätstheorie auf die Schwingung von Schützen. Doktor-Ingenieur dissertation, Universität Karlsruhe.

MARTIN, W. W., NAUDASCHER, E. & PADMANABHAN, M. 1975 Fluid-dynamic excitation involving flow instability. *Proc. A.S.C.E.* **101** (HY6), 681.

MICHALKE, A. 1971 Instabilität eines kompressiblen runden Freistrahls unter Berücksichtigung des Einflusses der Strahlgrenzschichtdichte. *Z. Flugwiss.* **19**, 319.

MUELLER, T. J. & LEARY, R. A. 1970 Physical and numerical experiments in laminar incompressible separating and reattaching flows. *A.I.A.A. Paper* no. 70–763.

OKA, S. & KOSTIC, Z. 1971 Influence of the wall proximity on the hot-wire velocity measurements. *Boris Kidric Inst. Nucl. Sci. Rep.* no. 1BK-1021. (See also *Proc. Int. Summer School on Heat and Mass Transfer in Boundary Layers, Beograd*, 1970.)

ROCKWELL, D. O. & NICCOLLS, W. O. 1972 Natural breakdown of planar jets. *A.S.M.E. Paper* no. 72-FE-5.

SATO, H. 1959 The stability and transition of a two-dimensional jet. *J. Fluid Mech.* **7**, 53.

SMYTH, R. 1976 Experimental study of turbulence in plane separated flows. *Proc. ISL/AGARD Workshop on Laser Anemometry*, p. 233.

WINANT, C. D. & BROWAND, F. K. 1974 Vortex pairing: the mechanism of turbulent mixing layer growth at moderate Reynolds number. *J. Fluid Mech.* **63**, 237.

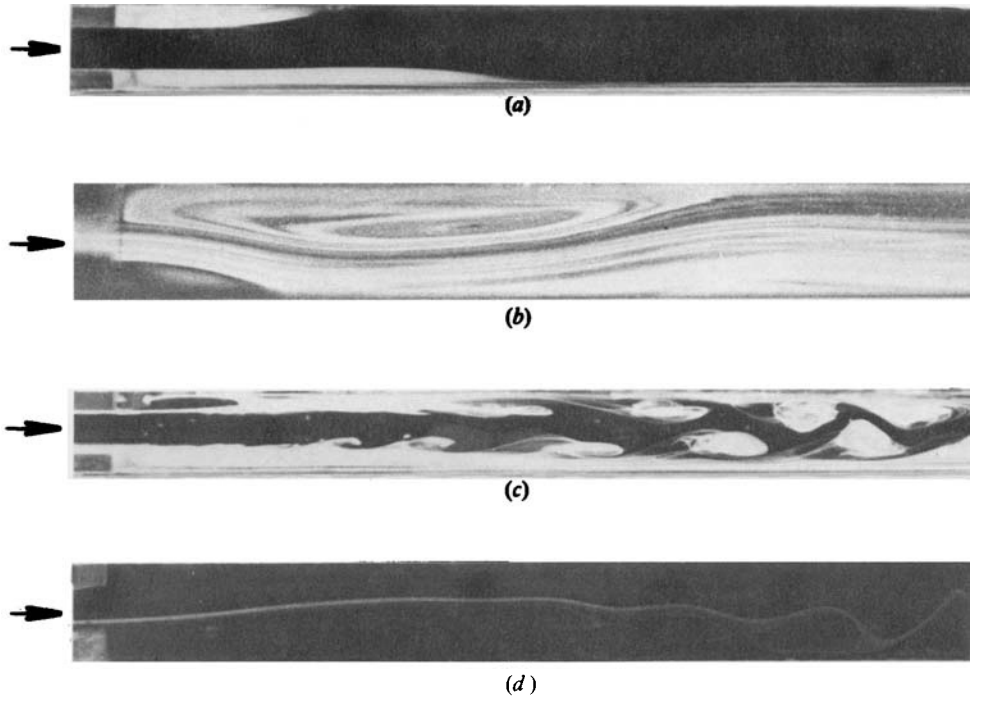

FIGURE 3. Flow-visualization techniques to obtain information on velocity field.

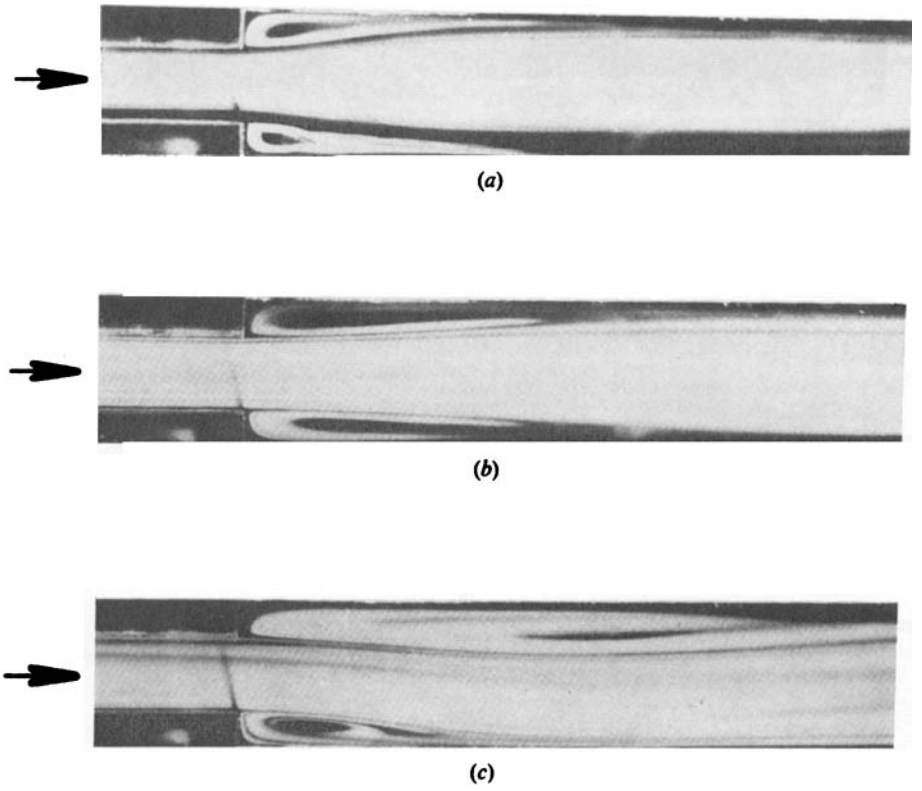

FIGURE 5. Flow patterns at different Reynolds numbers for an aspect ratio of 8 and an expansion ratio of 2. (*a*) $Re = 110$. (*b*) $Re = 150$. (*c*) $Re = 500$.

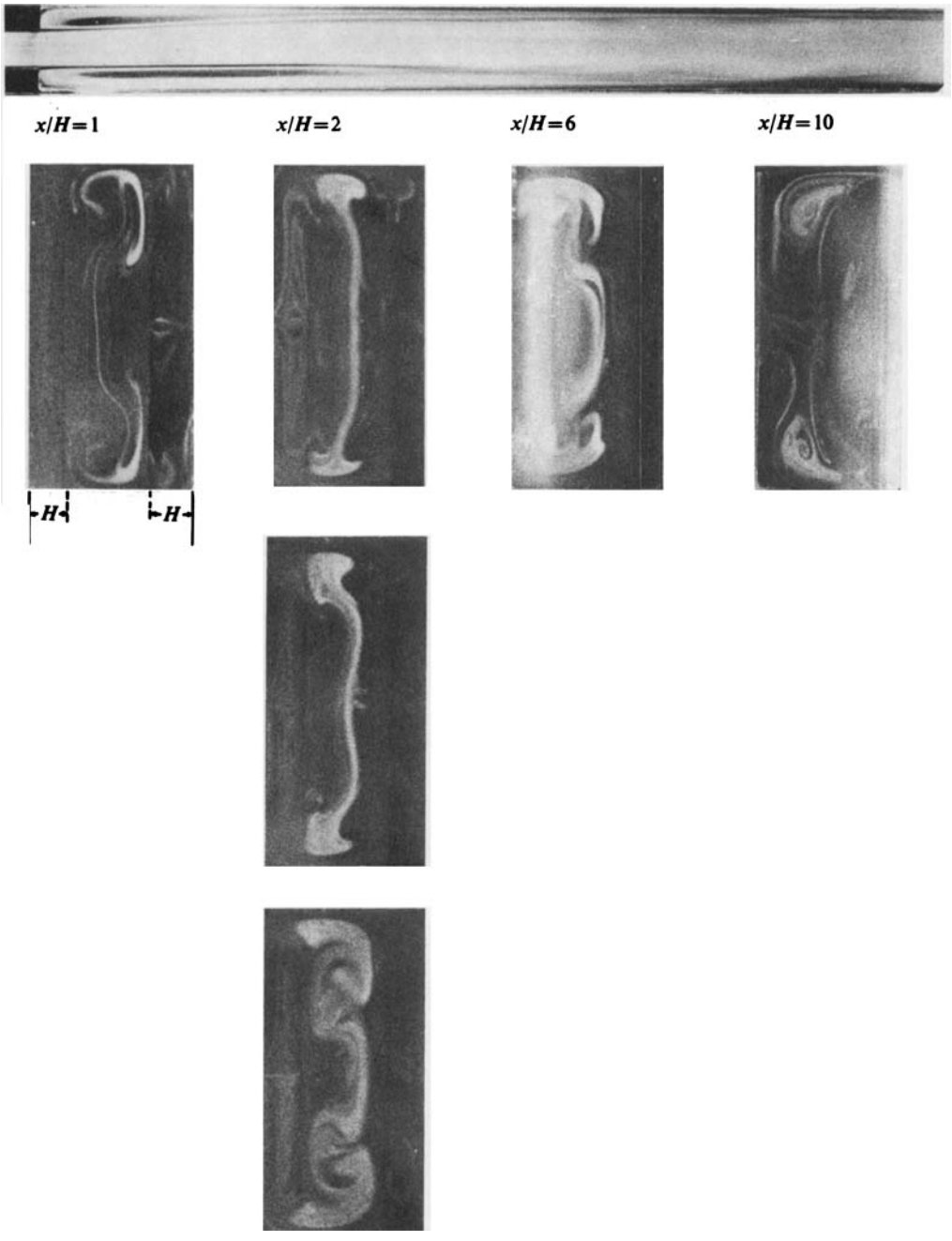

FIGURE 7. Typical smoke patterns of the recirculating flow (illumination in y, z plane).

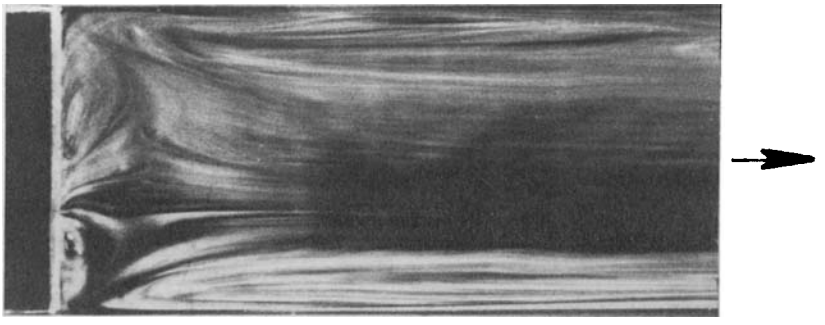

FIGURE 8. Typical smoke pattern of the recirculating flow (illumination in x, z plane).

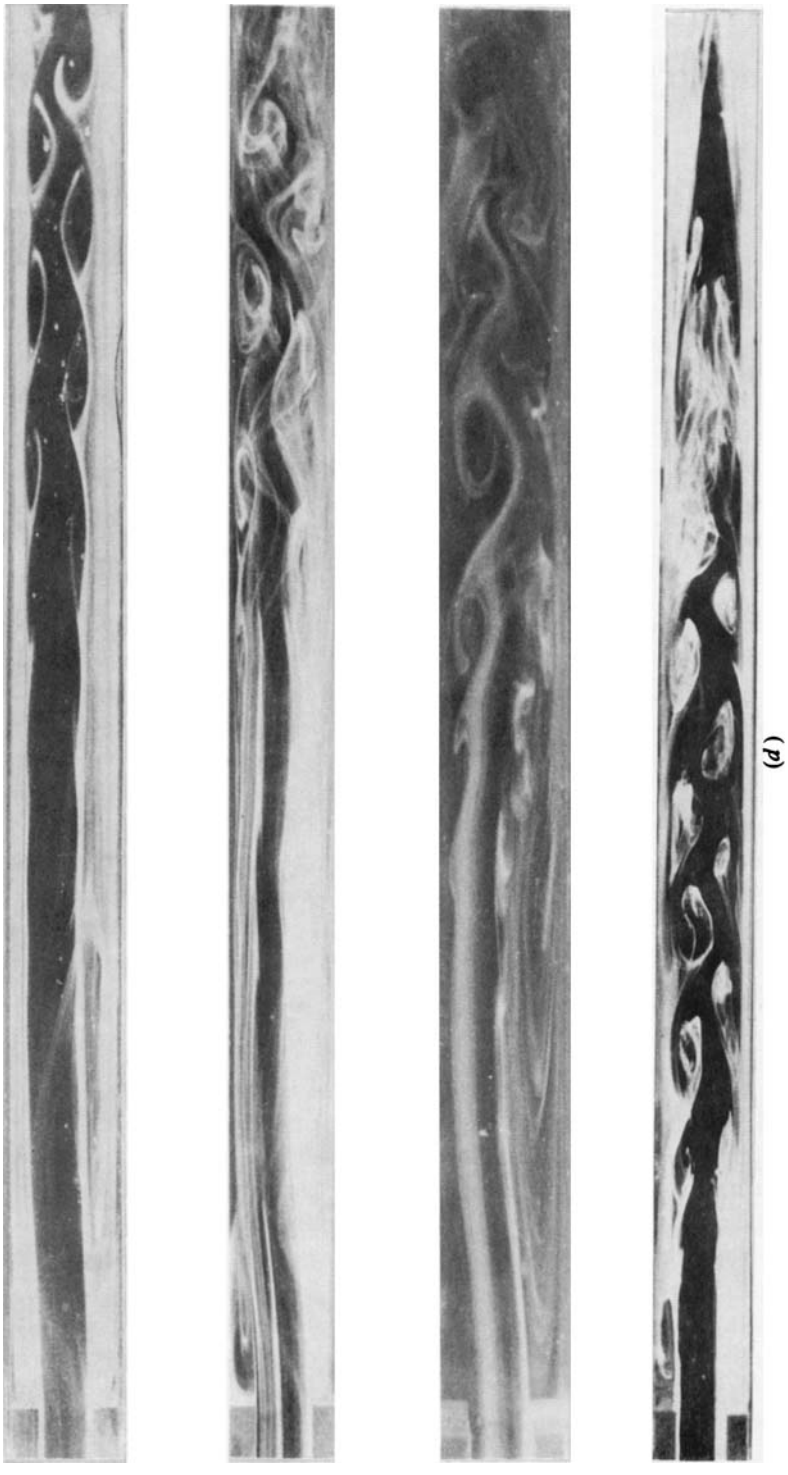

FIGURE 9. Examples of the formation of eddies for different geometrical and flow conditions. (*a*) Aspect ratio = 1, $Re = 1000$. (*b*) Aspect ratio = 2, $Re = 800$. (*c*) Aspect ratio = 4, $Re = 800$. (*d*) Aspect ratio = 8, $Re = 800$.